Atmospheric Environment 214 (2019) 116834

Contents lists available at ScienceDirect

Atmospheric Environment

journal homepage: www.elsevier.com/locate/atmosenv

Spatial variability and determinants of atmospheric methane concentrations in the metropolitan city of Shanghai, China

Min Liu[a,b,*], Ziqi Meng[a], Qiannan She[a], Xiyang Zhu[a], Ning Wei[c], Xia Peng[a], Qian Xu[a]

[a] Shanghai Key Laboratory for Urban Ecological Processes and Eco-Restoration, School of Ecological and Environmental Sciences, East China Normal University, Shanghai, 200241, PR China

[b] Institute of Eco-Chongming (IEC), Shanghai, 200062, PR China

[c] Shanghai Land Consolidation and Rehabilitation Center, Shanghai, 200003, PR China

ARTICLE INFO

Keywords:
Methane concentrations
Urban environment
Climate change
Shanghai

ABSTRACT

Methane, CH_4, is a powerful greenhouse gas released to the atmosphere by both anthropogenic and natural sources. Urban areas play an important role in greenhouse gas emissions, yet few efforts have been made to investigate CH_4 concentration and its spatial variability in cities. In this paper, a case study to monitor the spatial pattern and determinants of near-surface urban CH_4 concentration was conducted in Shanghai, the commercial and financial center of mainland China. A total of 173 sampling points were collected to examine the atmospheric CH_4 concentration across different land use types and urban-rural gradients at a height of 2 m above the ground in April and May 2014. The contributions of potential influencing factors, including four indicators of human activities (e.g., distance to natural gas pipelines [Dist_gas], distance to sewage plants [Dist_sew], population density [Den_pop], density of road network [Den_road]) and two indicators of natural conditions (i.e., planetary boundary layer height [BLH] and land surface temperature [LST]), in determining spatial CH_4 concentrations were investigated using Lindeman-Merenda-Gold (LMG) metric. The results indicated that the average CH_4 concentration in the morning for the region was 1,897 ± 92 parts per billion by volume (ppbv), with significant spatial heterogeneity. Atmospheric CH_4 had negative correlation with the distance to urban center except the influence of obvious emission sources, such as petrochemical plants etc. The six selected influencing factors could explain 76.3% of the CH_4 spatial variability. Population density was the dominant factor for about 27.2%, while the distance to the natural gas pipelines, planetary boundary layer height and distance to the sewage plants were about 14.4%, 14.2% and 12.6%, respectively. The finding in this study might help to build a better understanding of the mechanics of CH_4 variations and evaluation of the potentially influencing factors.

1. Introduction

Methane (CH_4) is a powerful long-lived greenhouse gas (GHG), with a global warming potential 34 times more potent than carbon dioxide (CO_2) over a period of 100 years (IPCC et al., 2014). Since the industrial revolution, atmospheric CH_4 concentration increased to reach a level of 1,853 ± 2 parts per billion by volume (ppbv), 257% higher than the pre-industrial level (~722 ppbv) mainly due to increased emissions from anthropogenic sources (WMO, 2017). Unlike atmospheric CO_2 with a steady increasing trend, global average atmospheric CH_4 has exhibited irregular anomalies of its inter-annual trends (Patra et al., 2009; NOAA, 2015). Global annual growth rate of CH_4 concentration showed the obvious fluctuation with a fast stage in the 1980s, a slowdown stage in the 1990s and a stable stage from 1999 to 2006 (Kirschke et al., 2013). Yet strong growth resumed in 2007 with an average annual growth rate of 0.3% (5 ppbv) (Dlugokencky et al., 2009; WMO, 2017). However, the reasons for these observed changes are still unclear (Saunois et al., 2016).

As a source-dependent GHG, it is vital to figure out how atmospheric CH_4 is balanced between sources and sinks. Previous studies have elucidated that methane sources can be categorized into two groups, namely, anthropogenic and natural sources (Wuebbles and Hayhoe, 2002; WMO, 2017). Anthropogenic sources include ruminants, rice agriculture, fossil fuel exploitations, landfills and biomass burning, which accounts for ~60% of the total methane emissions (Khalil et al., 1998; IPCC et al., 2014). Wetlands, lakes and rivers, oceans, termites,

* Corresponding author. Shanghai Key Laboratory for Urban Ecological Processes and Eco-Restoration, School of Ecological and Environmental Sciences, East China Normal University, Shanghai, 200241, PR China.
E-mail address: mliu@re.ecnu.edu.cn (M. Liu).

https://doi.org/10.1016/j.atmosenv.2019.116834
Received 22 June 2018; Received in revised form 5 July 2019; Accepted 12 July 2019
Available online 13 July 2019

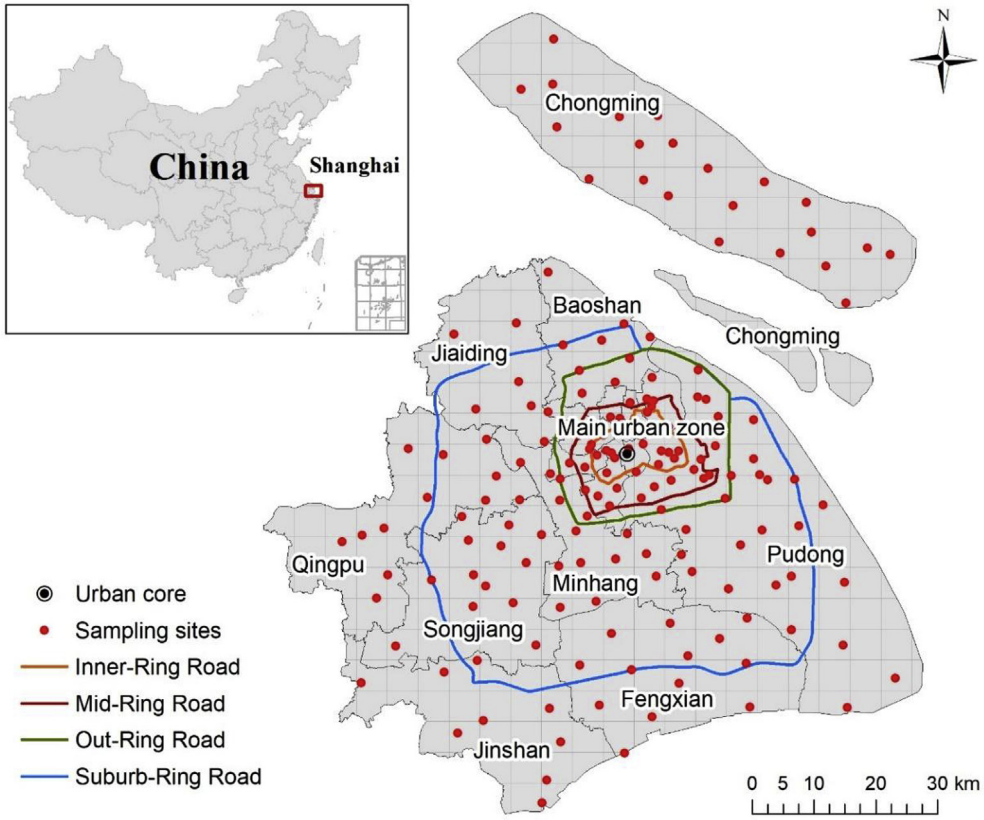

Fig. 1. Locations of sampling sites for CH_4 concentration in Shanghai (level of urbanization is defined by the ring roads).

hydrates and permafrost are considered as the natural sources of CH_4 (Conrad, 1999; Baldocchi et al., 2012). The removal of CH_4 is mediated by oxidation through OH radicals, which accounts for 90% of the total sinks (Kirschke et al., 2013). Furthermore, efforts have been made to estimate the global methane budget with inversion-based and process-based modeling methods (Bousquet et al., 2011; Zhu et al., 2014). However, due to the large spatial heterogeneity and temporal dynamics of CH_4, the regional model simulations of CH_4 budget were usually with large difference and inevitably suffered from deficiencies and uncertainties (Fraser et al., 2013). In-situ CH_4 measurements as well as discrete air samples are largely required to reduce such modeling uncertainties and in the forecast of future CH_4 levels (Kirschke et al., 2013).

Urban areas, the top energy and resource consumers to sustain the wellbeing of multitudes, are the main contributor to CH_4 rise in the atmosphere (Unger et al., 2006). However, most studies focused on CH_4 observation were located in undisturbed air with minimal influences of human activity (Fang et al., 2013; WMO, 2017), or areas dominated by biogenic fluxes and homogenous land use patterns, such as wetland and cropland (Desai et al., 2015; Martinez-Cruz et al., 2017). As a main source of GHGs, urban areas are projected to be frontiers in learning the impact of urbanization on the spatial patterns of atmospheric GHGs. However, studies in urban areas comprised of heterogeneous land cover have only widely studied during the past 20 years (Kim et al., 2010; Hopkins et al., 2016).

Recent studies carried out in urban areas focused on the direct measurement of CH_4 concentration, and fluxes based on eddy covariance over urban sites (Gioli et al., 2012; Morin et al., 2014). For CH_4 flux in urban areas, the published studies illustrated that a diurnal pattern existed during day time with a peak in the morning at 8:00. However, this fluctuation was relative small compared to that of CO_2 (Gioli et al., 2012). The nocturnal CH_4 fluxes were consistent and almost constant over time. Contrary to the CO_2, the surface fluxes of CH_4 did not reveal clear distinct seasonality (Zimnoch et al., 2010) or exhibited a moderate seasonality (Helfter et al., 2016). The exchange of CH_4 between the atmosphere and the underlying surface over urban areas is mostly governed by fugitive emissions from natural gas systems (Phillips et al., 2013; Hendrick et al., 2016), road traffic (Gioli et al., 2012), landfills (Sekhavatjou et al., 2012; Zazzeri et al., 2015) as well as biogenic and meteorological conditions including the presence of bacteria in urban soils (Groffman and Pouyat, 2009), wind speed (Morin et al., 2014), and atmospheric stability (Fang et al., 2013; Sanchez et al., 2014). To do these works, most studies of atmospheric CH_4 concentration in urban areas were mainly based on the continuous observations in fixed sites, which could obtain high temporal resolutions at the sacrifice of narrower spatial coverage (Gioli et al., 2012; Shen et al., 2014). However, these monitoring stations cannot accurately characterize the spatial variability in the surrounding area and thus may not be representative for the whole city. To get a more accurate picture of CH_4 concentration of urban areas, monitoring needs to be done after careful selection of the sites that cover a range of urbanization intensities, especially in the cities of developing countries with dense population and accelerating urbanization.

As the commercial and financial center of mainland China, Shanghai has been undergoing rapid urbanization as characterized by an accelerating growth in energy consumption during the last two decades. In this study, we aimed to understand the spatial variability and its controlling factors of atmospheric CH_4 at the full urban scale. To achieve this goal, observations of CH_4 concentration were conducted over 173 sampling sites across various land use types and urban-rural gradients. The influences of local human activities (e.g., population density, distance to natural gas pipelines etc.) and natural conditions (i.e., planetary boundary layer height and land surface temperature) on the spatial variability of CH_4 concentrations were also investigated.

2. Data and methods

2.1. Study area

Shanghai (30°40′-31°53′N, 120°51′-122°12′E) is a metropolitan city with a population up to 24.2 million (Shanghai Bureau of Statistics, 2017). The city is located in the Yangtze River Delta in East China, covering an area of 6,340.5 km^2 and has 16 county-level division (Fig. 1). It has a longitudinal extent of 120 km and a latitudinal extent of 100 km, with an average elevation of 4 m above the sea level. The meteorological condition in Shanghai is characterized by the marine monsoon subtropical climate with mean annual temperature of 17.7 °C and mean annual precipitation of 1,222.2 mm (Year, 2003–2015, data from Shanghai Meteorological Bureau).

In recent 40 years, Shanghai has experienced massive urbanization. Its urbanization rate has increased significantly from 59% since the Reform and Opening-Up era in 1978 to approximately 90% in 2013 (Shanghai Bureau of Statistics, 2014). Natural gas is the most common energy in Shanghai with a consumption of 6,472 million m^3 in 2012, nearly four times of its value in 2005. In addition, there are 2.3 billion m^3 sewage produced and 53 urban sewage treatment plants with a total processing capacity of 7.9 million m^3/day in Shanghai during 2014 (Fig. S1, Data from Shanghai Water Authority). On the other hand, the total area of wetland in Shanghai was 3,770 km^2, including 3,191 km^2 natural wetlands (i.e. marine/coastal wetlands, lake and river wetland), distributed in Qingpu, Pudong district, and Chongming, and 579 km^2 human-made wetlands (Data from the second wetland survey in Shanghai). The area with rice fields was 984 km^2 and the cattle stock of ruminant animals was 0.34 million units by the end of 2014.

2.2. Methodology for monitoring atmospheric methane

Sampling sites. Spatial heterogeneity of underlying surface structure and extreme roughness under urban environment are major challenges in monitoring atmospheric GHGs (Grimmond et al., 2002). In this study, a total number of 173 sample points were collected covering the whole urban area of Shanghai across urbanization gradients and various land use types, including transportation land use (TrLU), commercial land use (CoLU), agricultural land use (AgLU), green space land use (GrLU), educational land use (EduLU), residential land use (ResLU) and industrial land use (IndLU). Based on the officially issued document "The overall urban planning of Shanghai (Year, 1999–2020)", the urbanization level in Shanghai was determined according to the distance from main ring roads, namely heavy urbanization (H_urban, within Inner-Ring Rd), moderately heavy urbanization (MH_urban, outside Inner-Ring Rd and within Mid-Ring Rd), medium urbanization (M_urban, outside Mid-Ring Rd and within Outer-Ring Rd), moderately low urbanization (ML_urban, outside Out-Ring Rd and within Suburb-Ring Rd) and low urbanization (L_urban, outside Suburb-Ring Rd) (shown in Fig. 1).

As the spatial heterogeneity in highly urbanized areas was significantly higher than that in lower urbanized regions, multi-density stratified sampling methodology was used to determine the locations of sampling points. Specifically, the whole territory of Shanghai was first partitioned into 5 km × 5 km grids. The density of sampling points in urban regions was four times of the density in suburban areas. In highly urbanized areas, i.e., H_urban, MH_urban and M_urban, the proportion of point density assigned for three urban levels was 3:2:1. In less urbanized area (ML_urban and L_urban), the proportion was 2:1. The distribution of sampling points with respect to land use type and urbanization level was shown in Table 1.

Gas sampling strategy. Atmospheric stability have a great impact on the variability of greenhouse gas, especially in urban environment (Aikawa et al., 2006). In Shanghai, intensity of temperature inversion is considered as moderate in spring (0.93 °C per 100 m on 08:00 local standard time) (Yang et al., 2006). A study of temperature inversion of Shanghai from 1991 to 2009 by Zhu et al. (2014) indicated that the intensity of temperature inversion became significantly lower after 9:00–10:00 am compared to nocturnal situation. In addition, the morning rush hour in Shanghai started from 7:00 to 9:00. Gas sampling during 9:00–11:00 am may be less influenced by automobile exhausts. Therefore, we conducted in-situ measurements in the morning (9:00–11:00 am) of weekdays on sunny days with clear skies and calm winds, i.e., April 15, April 18, April 23–24, April 28–30, and May 4, 2014, to ensure a sufficient air circulation coupled with relative low traffic volume. At all sampling sites, monitoring was conducted at a height of 2 m above the ground (approximately 6 m above the sea level) at open areas. All air samples were collected through pre-vacuumed sample bags by using syringe equipped with three-way valve. During each sampling visit, triplicate air samples were collected. As it was very difficult to take samples at all 173 sampling points at once, we performed sampling at 20–24 sampling sites per day. More detailed information of the sampling could be found in Liu et al. (2016).

Table 1
Distribution of sampling points with respect to land use type and urbanization level ("/" means there is no sampling point).

Number of sampling sites	TrLU	CoLU	AgLU	RecLU	InsLU	ResLU	IndLU	Total
H_urban	2	7	/	2	2	4	/	17
MH_urban	3	6	/	2	4	4	2	21
M_urban	3	3	/	3	2	6	3	20
ML_urban	8	9	11	6	4	13	6	57
L_urban	12	8	17	7	3	5	6	58

Analysis with gas chromatography. Gas samples were analyzed by a 7890A gas chromatograph (Agilent Technologies Co. Ltd., USA), equipped with a flame ionization detector (FID) to detect CH_4 concentrations. The chromatograph analysis used a 2 m × 2 mm chromatograph column packed with XMS (60/80) with FID temperature of 200 °C and column temperature of 55 °C. The system was single-point calibrated with 2,000 ppbv CH_4 standards (Dalian Hede Technologies. Ltd., China) after measuring every six consecutive samples. System precision was less than 1% relative standard deviation at approximately ambient concentrations. During analysis, each gas sample was fully blended through syringe and immediately injected to the detector to ensure the accuracy of the measurement. According to our result of measurements, the bias for three parallels at each sampling site was within the range of 5–20 ppbv with 85.0% (147 out of 173 sampling sites) below 10 ppbv.

2.3. Characterizing relationships between CH_4 and potential factors

Urban areas are responsible for more than 70% of global anthropogenic greenhouse gas emissions from buildings, transport, industry, and waste-related sources (Grimm et al., 2008). The natural sources of methane include wetland, geologic and terrestrial sources. Fuel production, transport leakages, agricultural emissions, biomass burning and human waste-related emissions are the main anthropogenic sources of CH_4. Meanwhile, meteorological conditions exert direct influence in the atmospheric vertical diffusion and horizontal transport of greenhouse gas (Sreenivas et al., 2016). In this study, a set of 4 anthropogenic activity indicators and 2 meteorological conditions were selected to evaluate the influences of human activities and natural conditions on the variability of CH_4 across Shanghai. The distance to the natural gas pipelines (Dist_gas), the distance to the sewage plants (Dist_sew), population density (Den_pop) and density of road network (Den_road) were used to reflect the human activities. And the planetary boundary layer height (BLH) and land surface temperature (LST) were selected to reveal the meteorological conditions over the Shanghai.

Further, the relative importance of each potential factors in determining spatial CH_4 concentration was measured using Lindeman-

Merenda-Gold (LMG) metric with the "relaimpo" package in R software version 3.2.4 (Gromping, 2006). LMG computes the average contribution of each variable to the overall R^2 across all possible ordering and thus provides a unique decomposition of the explained variance when predictors are correlated. This method allows to differentiate the contribution of different correlated predictors in a multiple linear regression model (Gromping, 2006; Musavi et al., 2017). In order to reduce the effect of outliers and describe the relationship between CH_4 concentration and their influencing factors, we grouped the relevant factors and CH_4 into 15 bins according to CH_4 concentration with 30 ppbv as the interval. However, there was no data around 2150 ppbv and only one point around 2180 ppbv and 2210 ppbv.

2.4. Auxiliary data

2.4.1. Land cover data

The land cover data with a spatial resolution of 30 m were provided by the National Geomatics Centre of China (NGCC; Globeland30-2010: http://www.globalland-cover.com). Pixel-object-knowledge based approach was implemented on images from Landsat Thematic Mapper (TM), Enhanced Thematic Mapper plus (ETM+), and the HJ-1 (multispectral images of Chinese Environmental Disaster Alleviation Satellite), with a high accuracy of over 80% (Chen et al., 2015).

2.4.2. Population data

The population data in Shanghai were obtained from WorldPop datasets (http://www. worldpop.org.uk) (Fig. S2). This gridded population maps, whereby population numbers per 100 × 100 m grid square are estimated, represent a more consistent representation of population distributions across a landscape than administrative unit counts.

2.4.3. Road and traffic data

The road and traffic data for the study area was obtained from OpenStreetMap (http://download.geofabrik.de/asia/china.html) (Mooney et al., 2016), including urban expressways, highways, national roads, provincial roads, county roads and rural roads (Fig. S3).

2.4.4. Planetary boundary layer height

Weather and air quality are related to dynamic variations of planetary boundary layer processes (Vinogradova et al., 2007; Leventidou et al., 2013). The planetary boundary layer height (BLH) were an important meteorological parameter in studying the weather forecast and air pollution. In this study, the daytime BLH (9:00–11:00 am) was downloaded from the European Centre for Medium-Range Weather Forecasts (ECMWF; http://apps.ecmwf.int/datasets/data/interim-full-daily/levtype = sfc/), which was available at a 0.25 × 0.25 latitude-longitude resolution (Fig. S4).

2.4.5. Land surface temperature data

The MOD11A1 daily land surface temperature (LST) data were obtained from Moderate Resolution Imaging Spectroradiometer (MODIS) during the study period, with a spatial resolution of 1 km (Fig. S5). These data were obtained from the Level-1 and Atmosphere Archive & Distribution System (LAADS) Distributed Active Archive Center (DAAC) (https://ladsweb.modaps.eosdis.nasa.gov/).

3. Results and discussion

3.1. Spatial distribution of CH_4 concentrations over Shanghai

For Shanghai, the CH_4 concentration in the morning (09:00–11:00 am) during the study period varied from 1,784 to 2,177 ppbv, with an average value of 1,897 ± 92 ppbv. As shown in Fig. 2, there are clear differentiation in the spatial distribution of CH_4 concentrations over Shanghai. The highest CH_4 concentration of 2,177 ppbv was observed near a chemical plant (SINOPEC Shanghai Petrochemical Company) in the south edge. Conversely, the lowest value of 1,784 ppbv was observed on Chenhai road located in northwest edge of Chongming Island, which was far from the urban core. Furthermore, there were statistically significant difference in the average CH_4 concentrations between Chongming Island (1,838 ± 66 ppbv, N = 22) and mainland Shanghai (1,906 ± 916 ppbv, N = 151)($p < 0.001$). For Chongming Island, this could be partially related to the clean sea breeze that blew from the East China Sea that helped to form air circulation both horizontally and vertically, and thus lead the near-surface CH_4 to disperse more easily and react with tropospheric OH radicals. Overall, the spatial disparity in Shanghai (393 ppbv) was much higher than the amplitude of diurnal variation of atmospheric methane observed in regional background station at WMO/GAW of Lin'an (LAN) (45 ± 29 ppbv in spring during 2009–2011, Fang et al., 2013), situated approximately 150 km to the west of Shanghai in the Yangtze River Delta. This indicated that the spatial heterogeneity of methane concentrations in urban areas could be more meaningful and need to be paid more attention compared to the temporal dynamics.

The CH_4 concentrations from 173 sampling points were then interpolated through inverse distance weighting (IDW) interpolation provided by the ArcGIS 10.1. IDW interpolation is mathematical (deterministic) interpolation assuming closer values are more related than further values with its function. It assigns values to unknown points with a weighted average of the values available at the known points. As seen in Fig. 3, the highest CH_4 zone was located in the northeast edge of Baoshan District, which was mainly regulated by the superimposed effects of a nearby mega estuarine wetland and a natural gas industry. With static closed chamber-chromatograph method, CH_4 fluxes up to 1.00 mg m^{-2}·h^{-1} were observed over *Scirpus mariqueter* vegetation in Paotai Bay Wetland located in Baoshan District (Li et al., 2014). Shidongkou power plant (partially natural gas powered with 3 × 400 MW9F) located in this zone might be considered as emitters through leakages from pipelines, storage containers or routine venting, which are known fugitive methane emissions as reported in several cities in USA (Townsend-Small et al., 2012; Phillips et al., 2013; Jackson et al., 2014). With a survey of CH_4 emissions from 100 natural gas leaks in Metro Boston, MA, Hendrick et al. (2016) pointed out that the direct measures of CH_4 flux from individual leaks ranged from 4.0–2.3 × 10^4 g CH_4.day^{-1}. In addition, the high CH_4 values in the middle of Shanghai might be attributed to another natural gas powered electrical plant, Wujing power plant. Although Wujing power plant was yet under the process of transformation from old coal to new natural gas powered generator units, the pipelines and other infrastructures have already been built and in fully operation as a transfer station for transportation of natural gas as part of West-to-East Gas Transmission Pipe Line Project.

3.2. Variability of CH_4 across urbanization gradients and land use types

A linear function was developed to characterize the relationship between CH_4 concentration and distance from the urban core (DUC). As shown in Fig. 4, two measurements sampled close to major sources, i.e., one near the natural gas pipelines and another near the Shanghai Petrochemical Company, showed extreme high values. If we excluded these two points, namely with the adjusted datasets (CH_4_adj), the slope of the linear regression between CH_4 and DUC was −12.3 ppbv/km with a coefficient of determination (R^2) of 0.84. It could suggest that atmospheric CH_4 had negative correlation under the process of urbanization except the influence of obvious emission sources, such as landfills and petrochemical plants. As the complexity of the urban system, the applicability of the linear regression still needs to be verified with more observations in many other cities.

Fig. 4. Scatter plots of CH_4 concentrations against the corresponding distance to urban core (DUC). CH_4_adj indicated the adjusted result of linear regression when two measurements sampled close to major sources (red dots) were excluded from calculation. Black dotted line

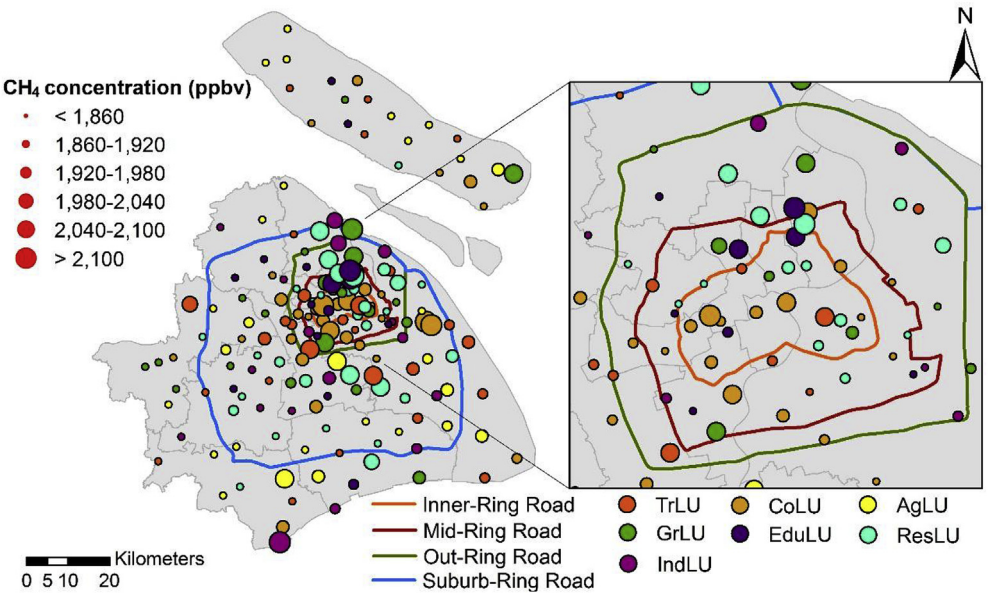

Fig. 2. Spatial distribution of CH_4 concentration in Shanghai with 173 sampling points.

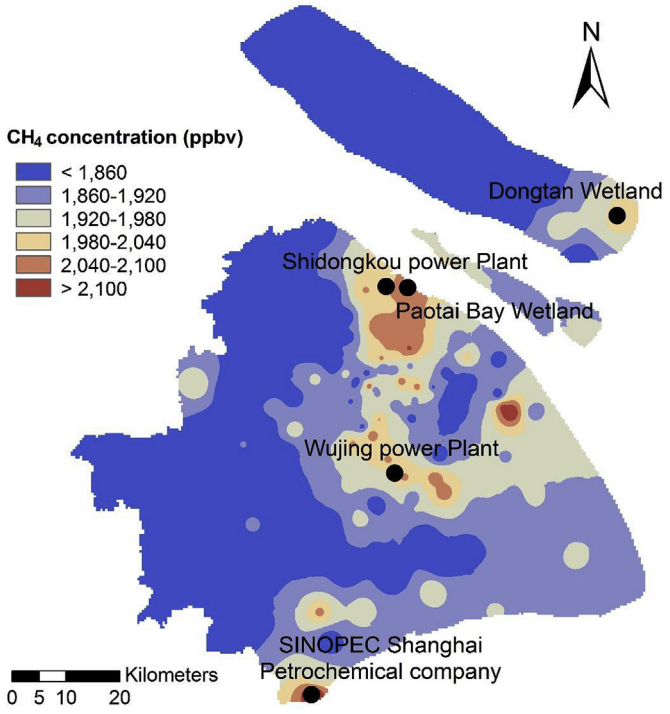

Fig. 3. Interpolated near-surface CH_4 concentration in Shanghai with Inverse Distance Weighting (IDW) interpolation.

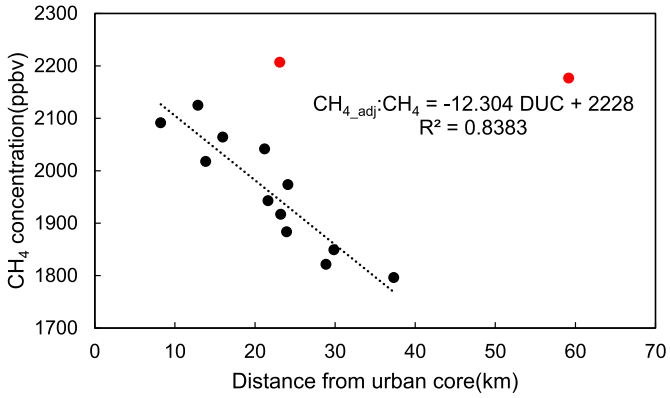

Fig. 4. Scatter plots of CH_4 concentrations against the corresponding distance to urban core (DUC). CH_{4_adj} indicated the adjusted result of linear regression when two measurements sampled close to major sources (red dots) were excluded from calculation. Black dotted line was the linear fitting curve of the ADJ regression. (For interpretation of the references to colour in this figure legend, the reader is referred to the Web version of this article.)

was the linear fitting curve of the CH_4_adj regression.

Furthermore, CH_4 concentrations appeared to differ significantly among different urbanization levels and land use types. To further explore the response of CH_4 concentrations to different urban development intensities, we grouped CH_4 based on urbanization intensity as shown in Table 2. Results also showed a decline trend of CH_4 concentrations on the whole as urbanization level dropped, with highest and lowest CH_4 concentration appeared in H_Urban (1,954 ± 88 ppbv) and L_Urban (1,874 ± 88 ppbv) urbanized areas, respectively. However, CH_4 concentrations in M_Urban (1,933 ± 107 ppbv) didn't match similar trend. This was partially due to the wide range of land uses occurred within M_Urban as well as sampling points that were significantly influenced by major sources in Baoshan District as previous mentioned. The average CH_4 concentrations in H_Urban and M_Urban were significantly higher than that in ML_Urban (1,883 ± 74 ppbv) and L_Urban ($p < 0.05$). It was worth to note that the variability of CH_4 concentration across urbanization gradients was not exactly the same with that of CO_2 (Liu et al., 2016). For CH_4, the highest value appeared in H_urban area, which may be related to the high population density. However, for CO_2, with the influence of both high residential density and activities in production, the highest CO_2 concentration occurred in moderate urbanization area rather than the high urbanization area.

As shown in Table 2, variations of CH_4 concentrations in different land use were illustrated. The averaged daytime CH_4 concentration varied from 1862 ± 106 ppbv in agricultural areas to 1924 ± 78 ppbv in commercial areas, whereas the CH_4 concentration was 1881 ppbv, 1897 ppbv, 1902 ppbv, 1911 ppbv, 1912 ppbv in the institute, industrial, transportation, recreational and residential areas, respectively. This result was consistent with studies in urban environment of Delhi (Padhy and Varshney, 2000; Sahay and Ghosh, 2013). Sahay and Ghosh (2013) reported significant gap between different land use types with

Table 2
CH_4 concentration over different urbanization levels and land use types.

CH_4	TrLU	CoLU	AgLU	RecLU	InsLU	ResLU	IndLU	Total
H_urban	1,974 ± 160	1,966 ± 107	/	1,916 ± 73	1,980 ± 101	1,928 ± 40	/	1,954 ± 88
MH_urban	1,889 ± 61	1,949 ± 105	/	2,053 ± 47	1,887 ± 120	1,918 ± 143	1,844 ± 37	1,923 ± 107
M_urban	1,943 ± 101	1,870 ± 31	/	1,908 ± 161	1,967 ± 189	1,951 ± 126	1,955 ± 57	1,933 ± 107
ML_urban	1,915 ± 78	1,888 ± 57	1,873 ± 76	1,857 ± 38	1,820 ± 23	1,906 ± 98	1,861 ± 49	1,883 ± 74
L_urban	1,869 ± 82	1,868 ± 58	1,855 ± 71	1,917 ± 119	1,832 ± 69	1,864 ± 68	1,924 ± 152	1,874 ± 88
Total	1,902 ± 86	1,925 ± 78	1,862 ± 72	1,911 ± 105	1,881 ± 106	1,912 ± 98	1,898 ± 98	1,897 ± 92

the highest mean concentration appeared in commercial areas (4,939 ± 1,340 ppbv), followed by residential (3,624 ± 1,715 ppbv), and industrial areas (1,115 ± 215 ppbv). The high CH_4 concentration in commercial areas could partially be related to the complex underlying surfaces, which could accumulate near-surface CH_4. While as a well-acknowledged major anthropogenic methane source through rice paddy and ruminants (Bousquet et al., 2006; Oo et al., 2015), the low CH_4 concentration in agricultural areas in this study area may be attributed to the location of the observation sites, most of which were near the coastlines with fine atmospheric circulation. Interestingly, standard deviations for authorized residential areas reached highest both in Delhi (1147–1299 ppbv, Sahay and Ghosh, 2013) and this study (105.7 ppbv). We attributed this phenomena to the sanitation facilities within the residential areas. Sanitation facilities, included sewers and dumping sites may differ significantly due to expense of maintaining fees, while such facilities in open air tend to generate more CH_4 compared to well-sealed ones.

3.3. Relevant factors affecting CH_4 concentrations

The land surface temperature (LST) in Shanghai during April to May 2014 ranged from 16.8 °C to 33.2 °C, which decreased with distance to the city center. The population density varied from the lowest of 0 in vegetation areas (e.g., farmland and grassland) to the highest in urban area-based built-up areas with 42,961 person/km^2. For the meteorological data, the atmospheric boundary layer height (BLH) obtained from ECMWF ranged from 294.2 m to 998.7 m, which was influenced by their distance to the coastline, the further away from the sea, the higher the BLH. The total length of major natural gas pipelines was about 646.9 km. The relationship between CH_4 and its relevant factors were shown in Fig. 5 and Table 3.

The spatial variability of CH_4 concentration in Shanghai depended largely on the distance to the natural gas pipelines (Dist_gas) with a negative correlation of 0.61 ($p < 0.05$). The result indicated that fugitive emissions from natural gas industries had significant impact on spatial pattern of atmospheric CH_4 concentrations. This finding was consistent with several similar studies (Phillips et al., 2013; Bamberger et al., 2014). Meanwhile, there was also a negative relationship between CH_4 and the distance to sewage plants ($r = -0.52$), although the correlation was not significant enough ($p < 0.1$). Within urban territory, anthropogenic activities such as natural gas industries, landfills, sewage treatments, cultivation of rice and ruminants were considered as major sources (Lowry et al., 2001; Kuc et al., 2003). Study from another megacity Seoul, Korea confirmed impacts of fugitive emissions on near-surface CH_4 concentrations (3.8 m above the ground level and 1 m from an 8-lane road) after implementation of natural gas powered vehicles. The CH_4 concentration increased by 180 ppbv compared to background level (Thi Nguyen et al., 2010). Accelerated consumption of natural gas might lead to rising risks of fugitive emissions through processing, transportation and storage of natural gas, thus it's vital to reduce fugitive emissions in order not to offset its comparative climate advantage (Phillips et al., 2013; Zazzeri et al., 2015).

For the meteorological conditions, there was a negative relationship between BLH and CH_4 ($r = -0.54$). The correlation between BC and BLH was consistent with that illustrated in Bechle et al. (2011), which

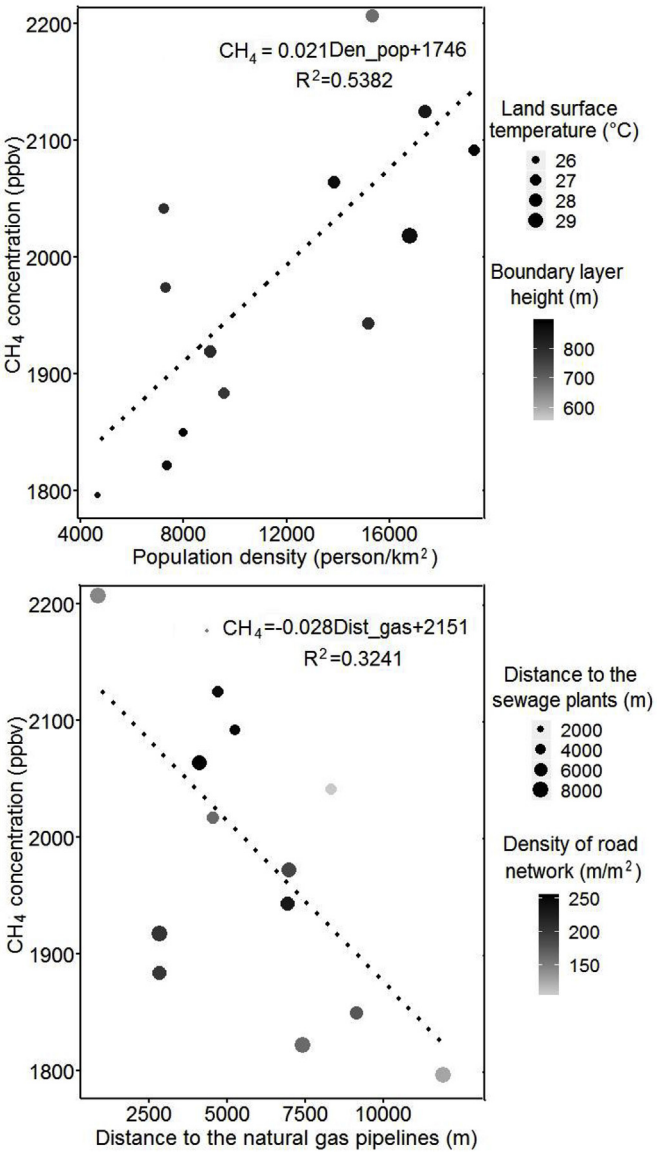

Fig. 5. Relationship of CH_4 with human activities and natural conditions. Den_pop: Population density (person/km^2); Dist_gas: Distance to the natural gas pipelines (m).

concluded that there was a significant negative correlation between atmospheric dilution rate and NO_2 concentrations measured from satellites. Numerous studies have shown that the sea-land breeze circulation enhances the atmospheric circulation in coastal cities (Fu and Tai, 2015; Wang et al., 2018). In addition, population density had a remarkably positive correlation with CH_4, with a correlation coefficients of 0.74 ($p < 0.01$). This showed that the larger population in the urban area, the greater the household energy consumption and the higher the CH_4 emissions, similar to the study by Huang et al. (2011)

Table 3
The correlation coefficients (r) among CH_4 and its relevant factors. The proportion of the CH_4 variance explained by the influencing factors with LMG metric was also illustrated.

	CH_4	Dist_gas	Dist_sew	BLH	LST	Den_Pop	Den_Road	Relative Contribution
CH_4	1.00	−0.61**	−0.52*	−0.54**	0.31	0.74***	0.15	76.3%(total)
Dist_gas		1.00	0.01	0.43	−0.55**	−0.57**	−0.34	14.4%
Dist_sew			1.00	0.33	0.15	−0.46	−0.04	12.6%
BLH				1.00	0.28	0.01	0.31	14.2%
LST					1.00	0.76***	0.33	5.2%
Den_Pop						1.00	0.61**	27.2%
Den_Road							1.00	2.8%

***$p < 0.01$ **$p < 0.05$ **$p < 0.1$.

and Wang et al. (2018). However, the relationship between road density and CH_4 was insignificant ($p > 0.05$), which indicated that the impact from traffic sources on CH_4 variability was very limited in the study area.

It was worth noting that the spatial CH_4 was not determined by one single factor, but the result of the combined effects of various relevant factors. Overall, spatial variability of atmospheric CH_4 under urban environment was controlled by complex interactions between location and intensity of methane sources (Phillips et al., 2013; Jackson et al., 2014), atmospheric stability, vertical mixing (Aikawa et al., 2006), local meteorological conditions (Sanchez et al., 2014) as well as land use types across urban gradients (Padhy and Varshney, 2000; Sahay and Ghosh, 2013). With the LMG method, the illustrated six influencing factors in this study could explain 76.3% of the CH_4 variability. Population density was the dominant factor for about 27.2%, while the distance to the natural gas pipelines, boundary layer height and distance to the sewage plant were about 14.4%, 14.2% and 12.6%, respectively (Table 3). The rest 23.7% CH_4 variability could be contributed by other meteorological conditions and anthropogenic emissions such as atmospheric transmission and biomass burning etc., which were not included in this study.

4. Conclusions

In this study, air sampling of near-surface atmospheric CH_4 was conducted at full urban scale in Shanghai, China. Based on measurements of 173 sampling sites, we examined the spatial variation of CH_4 concentrations and its variation across urbanization gradients and land use types. The relationships between CH_4 and natural environment and human activities were also studied and discussed. The average morning (9:00–11:00 am) CH_4 concentration in Shanghai was 1,897 ± 92 ppbv. Spatially, CH_4 concentrations were heterogeneously distributed with most high values located in the east part, which was mainly determined by the nearby local sources, especially fugitive emissions from natural gas industries, landfills and wetlands. A decline trend of CH_4 concentrations was found as urbanization level dropped. There was a significant negative relationship between CH_4 and the distance to the urban core, with a coefficient of determination (R^2) of 0.84, except the influence of obvious emission sources, such as landfills and petrochemical plants. The averaged daytime CH_4 concentration varied from 1,862 ± 106 ppbv in agricultural areas to 1,924 ± 78 ppbv in commercial areas. Further analysis indicated that the six selected factors, including two indicators of natural conditions and four indicators of human activities, could explain 76.3% of the CH_4 variability. Population density had a remarkably positive correlation with CH_4, with a correlation coefficient of 0.74 ($p < 0.01$), whereas the distance to the natural gas pipelines and sewage plants presented negative effects on the CH_4 concentration.

The temporal dynamics of CH_4 concentrations was very important for urban areas. However, in this study, we mainly focused on the CH_4 spatial variation with the sampling in the morning, with limited temporal representativeness. Meanwhile, the explaining factors illustrated in this study could not express the CH_4 spatial variability completely. In order to get comprehensive and objective investigation of CH_4 in urban areas, future studies should focus on performing CH_4 sampling along transects or continuous observation in common points with long-term observations and more explanatory variables in different urban areas.

Declaration of competing interest

The authors declare that they have no known competing financial interests or personal relationships that could have appeared to influence the work reported in this paper.

Acknowledgements

This work was supported by the Ministry of Science and Technology of the People's Republic of China (2017YFC0505800, 2016YFC0500204,2016YFC0208700), the Natural Science Foundation of Shanghai (17ZR1408700) and the National Natural Science Foundation of China (41471076). We would like to express our sincere gratitude to Dongqi Wang for the technical assistance with the measuring equipment as well as Shanghai Meteorological Bureau for kindly providing meteorological data. Many thanks to Dr. Varenyam Achal for polishing the English writing. We are also very grateful for five anonymous reviewers in providing invaluable suggestions and comments for this paper.

Appendix A. Supplementary data

Supplementary data to this article can be found online at https://doi.org/10.1016/j.atmosenv.2019.116834.

References

Aikawa, M., Hiraki, T., Eiho, J., 2006. Vertical atmospheric structure estimated by heat island intensity and temporal variations of methane concentrations in ambient air in an urban area in Japan. Atmos. Environ. 40, 4308–4315.
Bamberger, I., Stieger, J., Buchmann, N., Eugster, W., 2014. Spatial variability of methane: attributing atmospheric concentrations to emissions. Environ. Pollut. 190, 65–74.
Baldocchi, D., Detto, M., Sonnentag, O., Verfaillie, J., Teh, Y.A., Silver, W., Kelly, N.M., 2012. The challenges of measuring methane fluxes and concentrations over a peatland pasture. Agric. For. Meteorol. 153, 177–187.
Bechle, M.J., Millet, D.B., Marshall, J.D., 2011. Effects of income and urban form on urban NO2: global evidence from satellites. Environ. Sci. Technol. 45, 4914–4919.
Bousquet, P., Ciais, P., Miller, J.B., Dlugokencky, E.J., Hauglustaine, D.A., Prigent, C., Van der Werf, G.R., Peylin, P., Brunke, E.G., Carouge, C., Langenfelds, R.L., Lathiere, J., Papa, F., Ramonet, M., Schmidt, M., Steele, L.P., Tyler, S.C., White, J., 2006. Contribution of anthropogenic and natural sources to atmospheric methane variability. Nature 443, 439–443.
Bousquet, P., Ringeval, B., Pison, I., Dlugokencky, E.J., Brunke, E.G., Carouge, C., Chevallier, F., Fortems-Cheiney, A., Frankenberg, C., Hauglustaine, D.A., Krummel, P.B., Langenfelds, R.L., Ramonet, M., Schmidt, M., Steele, L.P., Szopa, S., Yver, C., Viovy, N., Ciais, P., 2011. Source Attribution of the Changes in Atmospheric Methane for 2006–2008. Atmos. Chem. Phys 11, 3689–3700.

Chen, J., Chen, J., Liao, A.P., Cao, X., Chen, L.J., Chen, X.H., He, C.Y., Han, G., Peng, S., Lu, M., Zhang, W.W., Tong, X.H., Mills, J., 2015. Global land cover mapping at 30 m resolution: a POK-based operational approach. ISPRS J. Photogrammetry Remote Sens. 103, 7–27.

Conrad, R., 1999. Contribution of hydrogen to methane production and control of hydrogen concentrations in methanogenic soils and sediments. FEMS (Fed. Eur. Microbiol. Soc.) Microbiol. Ecol. 28, 193–202.

Desai, A.R., Xu, K., Tian, H., Weishampel, P., Thom, J., Baumann, D., Andrews, A.E., Cook, B.D., King, J.Y., Kolka, R., 2015. Landscape-level terrestrial methane flux observed from a very tall tower. Agric. For. Meteorol. 201, 61–75.

Dlugokencky, E.J., Bruhwiler, L., White, J.W.C., Emmons, L.K., Novelli, P.C., Montzka, S.A., Masarie, K.A., Lang, P.M., Crotwell, A.M., Miller, J.B., Gatti, L.V., 2009. Observational constraints on recent increases in the atmospheric CH4 burden. Geophys. Res. Lett 36, L18803.

Fang, S.X., Zhou, L.X., Masarie, K.A., Xu, L., Rella, C.W., 2013. Study of atmospheric CH_4 mole fractions at three WMO/GAW stations in China. J. Geophys. Res. D Atmos. 118, 4874–4886.

Fraser, A., Palmer, P.I., Feng, L., Boesch, H., Cogan, A., Parker, R., Dlugokencky, E.J., Fraser, P.J., Krummel, P.B., Langenfelds, R.L., O'Doherty, S., Prinn, R.G., Steele, L.P., van der Schoot, M., Weiss, R.F., 2013. Estimating regional methane surface fluxes: the relative importance of surface and GOSAT mole fraction measurements. Atmos. Chem. Phys. 13, 5697–5713.

Fu, Y., Tai, A.P.K., 2015. Impact of climate and land cover changes on tropospheric ozone air quality and public health in east asia between 1980 and 2010. Atmos. Chem. Phys 15, 10093–10106.

Gioli, B., Toscano, P., Lugato, E., Matese, A., Miglietta, F., Zaldei, A., Vaccari, F.P., 2012. Methane and carbon dioxide fluxes and source partitioning in urban areas: the case study of florence, Italy. Environ. Pollut. 164, 125–131.

Groffman, P.M., Pouyat, R.V., 2009. Methane uptake in urban forests and lawns. Environ. Sci. Technol. 43, 5229–5235.

Grimm, N.B., Faeth, S.H., Golubiewski, N.E., Redman, C.L., Wu, J.G., Bai, X.M., 2008. Global change and the ecology of cities. Science 319, 756–760.

Grimmond, C.S.B., King, T.S., Cropley, F.D., Nowak, D.J., Souch, C., 2002. Local-scale fluxes of carbon dioxide in urban environments: methodological challenges and results from Chicago. Environ. Pollut. 1, S243–S254 116, Supplement.

Gromping, U., 2006. Relative importance for linear regression in R: the package relaimpo. J. Stat. Softw. 17.

Helfter, C., Tremper, A.H., Halios, C.H., Kotthaus, S., Bjorkegren, A., Grimmond, C.S.B., Barlow, J.F., Nemitz, E., 2016. Spatial and temporal variability of urban fluxes of methane, carbon monoxide and carbon dioxide above London, UK. Atmos. Chem. Phys. 16, 10543–10557.

Hendrick, M.F., Ackley, R., Sanaie-Movahed, B., Tang, X.J., Phillips, N.G., 2016. Fugitive methane emissions from leak-Prone natural gas distribution infrastructure in urban environments. Environ. Pollut. 213, 710–716.

Hopkins, F.M., Kort, E.A., Bush, S.E., Ehleringer, J.R., Lai, C.T., Blake, D.R., Randerson, J.T., 2016. Spatial patterns and source attribution of urban methane in the Los Angeles Basin. J. Geophys. Res. D Atmos. 121, 2490–2507.

Huang, C., Chen, C.H., Li, L., Cheng, Z., Wang, H.L., Huang, H.Y., Streets, D.G., Wang, Y.J., Zhang, G.F., Chen, Y.R., 2011. Emission inventory of anthropogenic air pollutants and VOC species in the Yangtze River Delta region, China. Atmos. Chem. Phys. 11, 4105–4120.

IPCC, 2014. Summary for policymakers. In: Stocker, T.F., Qin, D., Plattner, G.-K., Tignor, M., Allen, S.K., Boschung, J., Nauels, A., Xia, Y., Bex, V., Midgley, P.M. (Eds.), Climate Change 2013: the Physical Science Basis. Contribution of Working Group I to the Fifth Assessment Report of the Intergovernmental Panel on Climate Change. Cambridge University Press, Cambridge, United Kingdom and New York, NY, USA, pp. 714.

Jackson, R.B., Down, A., Phillips, N.G., Ackley, R.C., Cook, C.W., Plata, D.L., Zhao, K.G., 2014. Natural gas pipeline leaks across Washington, DC. Environ. Sci. Technol 48, 2051–2058.

Khalil, M.A.K., Rasmussen, R.A., Shearer, M.J., Dalluge, R.W., Ren, L.X., Duan, C.L., 1998. Measurements of methane emissions from rice fields in China. J. Geophys. Res. 103, 25181–25210.

Kim, D.-G., Isenhart, T.M., Parkin, T.B., Schultz, R.C., Loynachan, T.E., 2010. Methane flux in cropland and adjacent riparian buffers with different vegetation covers. J. Environ. Qual. 39, 97–105.

Kirschke, S., Bousquet, P., Ciais, P., Saunois, M., Canadell, J.G., Dlugokencky, E.J., Bergamaschi, P., Bergmann, D., Blake, D.R., Bruhwiler, L., Cameron-Smith, P., Castaldi, S., Chevallier, F., Feng, L., Fraser, A., Heimann, M., Hodson, E.L., Houweling, S., Josse, B., Fraser, P.J., Krummel, P.B., Lamarque, J.F., Langenfelds, R.L., Le Quere, C., Naik, V., O'Doherty, S., Palmer, P.I., Pison, I., Plummer, D., Poulter, B., Prinn, R.G., Rigby, M., Ringeval, B., Santini, M., Schmidt, M., Shindell, D.T., Simpson, I.J., Spahni, R., Steele, L.P., Strode, S.A., Sudo, K., Szopa, S., van der Werf, G.R., Voulgarakis, A., van Weele, M., Weiss, R.F., Williams, J.E., Zeng, G., 2013. Three decades of global methane sources and sinks. Nat. Geosci. 6, 813–823.

Kuc, T., Rozanski, K., Zimnoch, M., Necki, J.M., Korus, A., 2003. Anthropogenic Emissions of CO2 and CH4 in an Urban Environment. Appl.d Energy, vol. 75, 193–203.

Leventidou, E., Zanis, P., Balis, D., Giannakaki, E., Pytharoulis, I., Amiridis, V., 2013. Factors affecting the comparisons of planetary boundary layer height retrievals from CALIPSO, ECMWF and radiosondes over Thessaloniki, Greece. Atmos. Environ. 74, 360–366.

Liu, M., Wu, J., Zhu, X., He, H., Jia, W., Xiang, W., 2016. Spatial variation of near-surface CO2 concentration during Spring in Shanghai. Atmos Pollut. Res 7, 31–39.

Li, Y., Chen, Z., Wang, D., Hu, H., Wang, C., 2014. The study of methane emission in the process of wetland vegetation succession in Yangtze estuary salt marsh. Acta Sci. Circumstantiae 08, 2035–2042 (in Chinese).

Lowry, D., Holmes, C.W., Rata, N.D., O'Brien, P., Nisbet, E.G., 2001. London methane emissions: use of diurnal changes in concentration and δ13C to identify urban sources and verify inventories. J. Geophys. Res. 106, 7427–7448.

Martinez-Cruz, K., Gonzalez-Valencia, R., Sepulveda-Jauregui, A., Plascencia-Hernandez, F., Belmonte-Izquierdo, Y., Thalasso, F., 2017. Methane emission from aquatic ecosystems of Mexico City. Aquat. Sci. 79, 159–169.

Mooney, P., Minghini, M., Laakso, M., Antoniou, V., Olteanu-Raimond, A.M., Skopeliti, A., 2016. Towards a protocol for the collection of VGI vector data. ISPRS Int. J. Geo-Inf. 5, 217.

Morin, T.H., Bohrer, G., Frasson, R.P.D.M., Naor-Azreli, L., Mesi, S., Stefanik, K.C., Schafer, K.V.R., 2014. Environmental drivers of methane fluxes from an urban temperate wetland park. J. Geophys. Res.: Biogeosciences 119, 2188–2208.

Musavi, T., Migliavacca, M., Reichstein, M., Kattge, J., Wirth, C., Black, T.A., Janssens, I., Knohl, A., Loustau, D., Roupsard, O., Varlagin, A., Rambal, S., Cescatti, A., Gianelle, D., Kondo, H., Tamrakar, R., Mahecha, M.D., 2017. Stand age and species richness dampen interannual variation of ecosystem-level photosynthetic csapacity. Nat.Ecol. Evol. 1.

NOAA (National Oceanic and Atmospheric Administration), 2015. Trends in atmospheric carbon dioxide. Available at: http://www.esrl.noaa.gov/gmd/ccgg/trends/.

Oo, A.Z., Win, K.T., Bellingrath-Kimura, S.D., 2015. Within Field Spatial Variation in Methane Emissions from Lowland Rice in Myanmar. Springerplus4.

Padhy, P.K., Varshney, C.K., 2000. Ambient methane levels in Delhi. Chemosphere Global Change Sci. 2, 185–190.

Patra, P.K., Takigawa, M., Ishijima, K., Choi, B.C., Cunnold, D., Dlugokencky, E.J., Fraser, P., Gomez-Pelaez, A.J., Goo, T.Y., Kim, J.S., Krummel, P., Langenfelds, R., 2009. Growth rate, seasonal, synoptic, diurnal variations and budget of methane in the lower atmosphere. J. Meteorol. Soc. Jpn. 87, 635–663.

Phillips, N.G., Ackley, R., Crosson, E.R., Down, A., Hutyra, L.R., Brondfield, M., Karr, J.D., Zhao, K.G., Jackson, R.B., 2013. Mapping urban pipeline leaks: Methane leaks across Boston. Environ. Pollut. 173, 1–4.

Sahay, S., Ghosh, C., 2013. Monitoring variation in greenhouse gases concentration in urban environment of delhi. Environ. Monit. Assess. 185, 123–142.

Sanchez, M.L., Garcia, M.A., Perez, I.A., Pardo, N., 2014. CH4 continuous measurements in the upper spanish plateau. Environ. Monit. Assess. 186, 2823–2834.

Saunois, M., Jackson, R.B., Bousquet, P., Poulter, B., Canadell, J.G., 2016. The growing role of methane in anthropogenic climate change. Environ. Res. Lett. 11, 120207.

Sekhavatjou, M.S., Mehdipour, A., Takdastan, A., Alhashemi, A.H., 2012. CH_4 and total GHGs emission from urban landfills in southwest Iran. J. Integr. Environ. Sci. 9, 217–223.

Shanghai Bureau of Statistics, 2014. Shanghai Statistical Yearbook 2013. China Statistics Press, Beijing.

Shanghai Bureau of Statistics, 2017. Shanghai Statistical Yearbook 2016. China Statistics Press, Beijing.

Shen, S., Yang, D., Xiao, W., Liu, S., Lee, X., 2014. Constraining anthropogenic CH_4 emissions in Nanjing and the Yangtze River Delta, China, using atmospheric CO_2 and CH_4 mixing ratios. Adv. Atmos. Sci. 31, 1343–1352.

Sreenivas, G., Mahesh, P., Subin, J., Kanchana, A.L., Rao, P.V.N., Dadhwal, V.K., 2016. Influence of Meteorology and interrelationship with greenhouse gases (CO_2 and CH_4) at a suburban site of India. Atmos. Chem. Phys. 16, 3953–3967.

Thi Nguyen, H., Kim, K.H., Ma, C.J., Cho, S.J., Ryeul Sohn, J., 2010. A dramatic shift in CO and CH_4 levels at urban locations in Korea after the implementation of the Natural Gas Vehicle Supply (NGVS) program. Environ. Res. 110, 396–409.

Townsend-Small, A., Tyler, S.C., Pataki, D.E., Xu, X., Christensen, L.E., 2012. Isotopic measurements of atmospheric methane in Los Angeles, California, USA: influence of "fugitive" fossil fuel emissions. J. Geophys. Res.: Atmosphere 117, D07308.

Unger, N., Shindell, D.T., Koch, D.M., Amann, M., Cofala, J., Streets, D.G., 2006. Influences of man-made emissions and climate changes on tropospheric ozone, methane, and sulfate at 2030 from a broad range of possible futures. J. Geophys. Res.: Atmosphere 111, D12313. https://doi.org/10.1029/2005JD006518.

Vinogradova, A.A., Fedorova, E.I., Belikov, I.B., Ginzburg, A.S., Elansky, N.F., Skorokhod, A.I., 2007. Temporal variations in carbon dioxide and methane concentrations under urban conditions. Izv. Atmos. Ocean. Phys. 43, 599–611.

Wang, Y., Du, H., Xue, Y., Lu, D., Wang, X., Guo, Z., 2018. Temporal and spatial variation relationship and influence factors on surface urban heat island and ozone pollution in the Yangtze River Delta, China. Sci. Total Environ. 631–632, 921–933.

WMO (World Meteorological Organization), 2017. Greenhouse Gas Bulletin: the State of Greenhouse Gases in the Atmosphere Based on Global Observations through 2016. World Meteorological Organization, Geneva.

Wuebbles, D.J., Hayhoe, K., 2002. Atmospheric methane and global change. *Earth* Sci. Rev. 57, 177–210.

Yang, Y., Tan, J., Zheng, Y., Cheng, S., 2006. Study on the atmospheric stabilities and the thickness of atmospheric mixed layer during recent 15 years in Shanghai. Scientia meteorologica sinica 26, 536–541 (in Chinese).

Zazzeri, G., Lowry, D., Fisher, R.E., France, J.L., Lanoiselle, M., Nisbet, E.G., 2015. Plume mapping and isotopic characterisation of anthropogenic methane sources. Atmos. Environ. 110, 151–162.

Zhu, X., Zhuang, Q., Lu, X., Song, L., 2014. Spatial scale-dependent land–atmospheric methane exchanges in the northern high latitudes from 1993 to 2004. Biogeosciences 11, 1693–1704.

Zimnoch, M., Godlowska, J., Necki, J.M., Rozanski, K., 2010. Assessing Surface Fluxes of CO2 and CH4 in Urban Environment: a Reconnaissance Study in Krakow, Southern Poland. Tellus Ser. B Chem. Phys. Meteorol. 62, 573–580.